Population of positive-parity states in ^{53}Sc through one-proton knockout

S. McDaniel,[1,2] A. Gade,[1,2] R. V. F. Janssens,[3] D. Bazin,[1] B. A. Brown,[1,2] C. M. Campbell,[1,2] M. P. Carpenter,[3] J. M. Cook,[1,2] A. N. Deacon,[4] D.-C. Dinca,[1,2] S. J. Freeman,[4] T. Glasmacher,[1,2] P. G. Hansen,[1,2] B. P. Kay,[4] P. F. Mantica,[1,5] W. F. Mueller,[1] J. R. Terry,[1,2] J. A. Tostevin,[6] and S. Zhu[3]

[1]*National Superconducting Cyclotron Laboratory, Michigan State University, East Lansing, Michigan 48824, USA*
[2]*Department of Physics and Astronomy, Michigan State University, East Lansing, Michigan 48824, USA*
[3]*Physics Division, Argonne National Laboratory, Argonne, Illinois 60439, USA*
[4]*School of Physics and Astronomy, Schuster Laboratory, University of Manchester, Manchester M13 9PL, United Kingdom*
[5]*Department of Chemistry, Michigan State University, East Lansing, Michigan 48824, USA*
[6]*Department of Physics, Faculty of Engineering and Physical Sciences, University of Surrey, Surrey GU2 7XH, United Kingdom*

The one-proton knockout reaction ^{9}Be(^{54}Ti, ^{53}Sc + γ)X at 72 MeV/nucleon has been measured. The location of the first $3/2^-$ state at 2110(3) keV was confirmed, and new γ-ray transitions were observed at 1111(2), 1273(2), 1539(4), and 2495(5) keV. Large spectroscopic strength to excited states in ^{53}Sc was found and attributed to the knockout of sd-shell protons.

I. INTRODUCTION

Knockout reactions are a well-established tool for probing the single-particle structure of exotic nuclei with large proton-neutron asymmetry [1,2]. In the collision with a light target, typically ^{9}Be or ^{12}C, the direct removal of a nucleon from a projectile nucleus with mass number A leads preferentially to the population of single-hole configurations in the mass $A - 1$ residue. The selective excitation of single-particle degrees of freedom, together with the connection between the initial state and the residue's final states in terms of wave-function overlaps, provides insight into the decomposition of the projectile's ground-state wave function in its single-particle components. This approach has allowed tracking of unexpected structural phenomena in exotic nuclei such as the existence of nuclear halos, the weakening and disappearance of canonical magic numbers, and the emergence of new shell gaps. For example, the region of neutron-rich Ne, Na, and Mg isotopes—the so-called Island of Inversion—where neutron particle-hole excitations across the $N = 20$ shell gap are energetically favored over normal-order shell filling [3], was investigated with this approach. The measured spectroscopic strength and the deduced orbital angular momentum, ℓ, of the removed nucleon quantified the presence of fp-shell neutron intruder configurations in the ground-state wave functions for ^{26,28}Ne and ^{30,32}Mg [4,5].

Similarly, for even-even projectiles, the knockout of a nucleon from a shell below the Fermi surface will populate cross-shell excitations in the residue, most often with a parity opposite to that of the residue's ground state. Through the knockout of these more deeply bound, nonvalence nucleons, the evolution of single-particle orbits that are often not included in the model spaces of shell-model calculations can be tracked. Thus these reactions underscore the need for cross-shell effective interactions and assist in their development. The region of neutron-rich Cr, Ti, and Ca isotopes with neutron numbers around $N = 32, 34$ has attracted much attention in recent years. The weakening of the $\pi f_{7/2}$-$\nu f_{5/2}$

proton-neutron monopole interaction, as protons are removed from the $f_{7/2}$ orbital, combined with a sizable neutron $p_{1/2}$-$p_{3/2}$ spin-orbit splitting, results in the emergence of an $N = 32$ subshell closure [6–10] in these isotopic chains. For Ca, the possibility of an $N = 34$ gap has been contemplated as well.

In contrast with the situation in its neutron-rich even-mass neighbors, little spectroscopic information was available for ^{53}Sc until recently. A lower limit for the half-life was proposed in Ref. [11] from an experiment at Grand Accélérateur National d'Ions Lourds (GANIL). More recent β-decay studies at the National Superconducting Cyclotron Laboratory (NSCL) began to elucidate the structure of ^{53}Sc in more detail [12]. The first excited $3/2^-$ state in ^{53}Sc was established at 2109 keV [12]. In a shell-model picture, this state is attributed to the coupling of a $\pi f_{7/2}$ valence proton with the 2_1^+ excited state of ^{52}Ca [^{52}Ca(2_1^+) $\otimes$ $\pi f_{7/2}$], forming a multiplet of five states, of which the $3/2^-$ state is lowest in energy. Further spectroscopy of ^{53}Sc was performed at GANIL using deep-inelastic, multinucleon transfer reactions [13]. New γ-ray transitions were observed at 345(7), 2283(18), and 2617(20) keV. The 2283- and 2617-keV decays were assigned to higher-lying $9/2^-$ and $11/2^-$ yrast states, with the 345-keV decay connecting the levels. These higher-spin states are also attributed to the $3/2^-$-$11/2^-$ quintet. For this article, the one-proton knockout reaction ^{9}Be(^{54}Ti, ^{53}Sc + γ)X at 72 MeV/u was used to probe the single-particle structure of this $N = 32$ nucleus.

II. EXPERIMENT AND RESULTS

The data presented here were obtained from a measurement dedicated primarily to properties of ^{52}Ca as obtained in a two-proton knockout reaction [14], and the reader is referred to the latter work for additional information. A secondary beam containing ^{54}Ti was produced in-flight at the NSCL. The large-acceptance A1900 fragment separator [15] was

used to select fragments of interest from the products created in the collision of a 130 MeV/u ^{76}Ge primary beam with a 423-mg/cm^2 ^{9}Be production target. A 300-mg/cm^2-thick achromatic Al wedge at the image of the A1900 further optimized the purity of ^{54}Ti in the beam. Two acceptance settings of the separator were employed, one with 1% total momentum acceptance for cross section measurements and another with no momentum restriction in the A1900 for γ-ray spectroscopy (the momentum bite transmitted to the experiment is limited to 4% by the acceptance of the S800 analysis beam line in focused optics). The ^{54}Ti purity in the secondary beam at 1% momentum acceptance was about 36%; the other two significant components in the projectile beam were ^{55}V and ^{57}Cr.

The ^{54}Ti secondary beam impinged on a 376(4)-mg/cm^2 ^{9}Be target located at the target position of the S800 spectrograph [16] with a mid-target energy of 72 MeV/u. A pair of thin plastic scintillators, located at the A1900 extended focal plane and at the object point of the S800 analysis line, identified the incoming projectiles through the time of flight. For the 1% total momentum acceptance, the magnetic rigidity of the S800 spectrograph was set to center ^{53}Sc in the focal plane. The setting without momentum restriction was optimized for two-proton knockout to ^{52}Ca [14], and the ^{53}Sc residues only entered the focal plane at the edge of the acceptance. The S800 focal-plane detection system provided energy-loss measurements, timing information, and positions and angles of the projectile-like reaction residues [17]. An example of the particle identification is given in Fig. 1.

The ^{9}Be reaction target was surrounded by the Segmented Germanium Array (SeGA) [18] of 17, 32-fold segmented germanium detectors, arranged in two rings at angles of 37° and 90° with respect to the beam axis. The high degree of segmentation provided the angular resolution necessary to

correct the γ rays emitted in-flight ($v/c \approx 0.4$) for the Doppler shifts. In this experiment, the angular opening of a SeGA segment (about 2.5°) is not the limiting contribution to the in-beam γ-ray energy resolution; the main contribution was the thick target and the resulting uncertainty in the beam velocity at the time of the γ-ray emission. The energy-dependent full-energy peak efficiency of the array was determined with standard calibration sources at rest and corrected for the Lorentz boost arising from the γ-ray emission in-flight (i.e., in-beam full-energy peak efficiencies of 2.8% at 1.1 MeV and 1.76% at 2.11 MeV were determined). SeGA was operated in coincidence with the S800 focal-plane detectors, allowing event-by-event correlation of the deexcitation γ rays with the ^{53}Sc knockout residues.

The Doppler-corrected γ-ray spectrum measured in coincidence with ^{53}Sc is presented in Fig. 2. This measurement confirms the presence of the 2109-keV transition ($3/2_1^- \rightarrow 7/2_{gs}^-$) reported in Ref. [12]. New γ-ray transitions were observed at 1111(2), 1273(2), 1539(4), and 2459(5) keV (see Fig. 2). The reported uncertainties include contributions associated with peak-fitting procedures as well as with the undetermined location and velocity of the ^{53}Sc products at the time of γ decay. We note that the nonobservation of the previously reported γ-ray transitions from the $11/2^-$ and $9/2^-$ core-coupled states reported in Ref. [13] is consistent with the one-step, direct one-proton knockout from the 0^+ ground state of ^{54}Ti, which selectively populates proton-hole states.

An inclusive cross section for the one-proton knockout reaction ^{9}Be(^{54}Ti,^{53}Sc)X of $\sigma = 17.6(6)$ mb was derived.
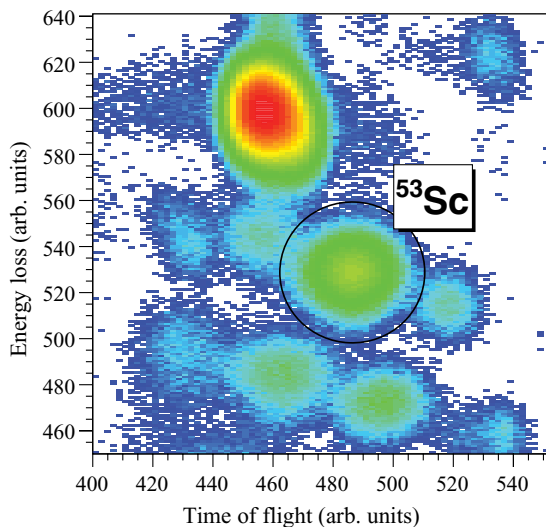

FIG. 1. (Color online) Particle identification in the S800 focal plane. The most intense contribution to this spectrum originates from ^{54}Ti^{+21}, that is, projectiles converted to a hydrogen-like charge state by passing through the target. The spectrum shows only events originating from identified ^{54}Ti projectiles in the incoming beam.
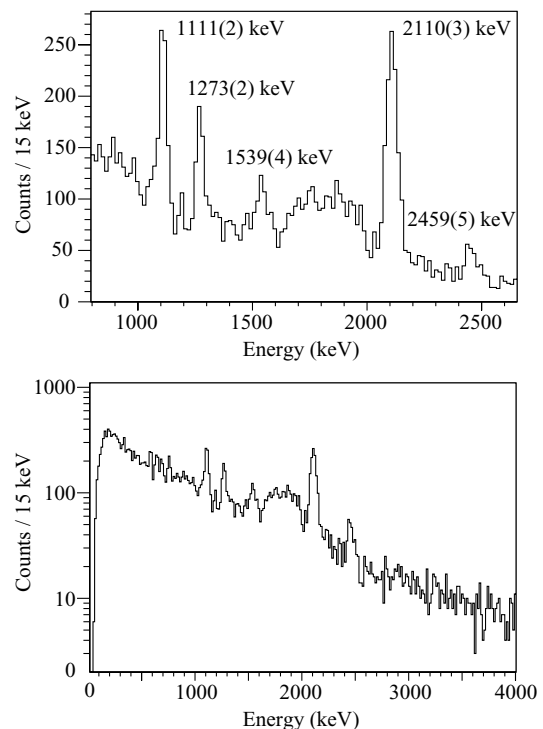

FIG. 2. Doppler-reconstructed γ-ray spectrum detected in coincidence with ^{53}Sc. Aside from the 2110-keV transition reported previously [12], all observed γ rays are new. There is no evidence for γ-ray transitions outside the displayed region.

Systematic errors of 3% from the stability of the cocktail-beam composition, of 1% from uncertainties on the acceptance corrections, and of 1% from the uncertainty in the target thickness were added to the statistical uncertainty and are included in the quoted accuracy. The cross sections for the population of individual final states can only be determined from ^{53}Sc parallel-momentum distributions located fully within the S800 acceptance (see, e.g., Ref. [1]). As indicated earlier, this requirement was not met here as the high-statistics γ-S800 coincidence measurement (Fig. 2) was carried out with settings optimized for ^{52}Ca [14]. Data on partial cross sections could be obtained only for the $3/2_1^-$ level as only the 2110-keV γ ray had sufficient intensity with ^{53}Sc centered in the focal plane. The spectroscopic strength obtained in this way includes the contribution of feeding by higher-lying states. To obtain the partial cross sections for the direct population of individual states, the indirect feeding has to be subtracted according to the decay level scheme, which was not possible in this experiment.

In the same way that the two-proton knockout reaction from ^{54}Ti proceeds through the removal of a pair of $f_{7/2}$ protons and feeds primarily ($\approx$70%) the ground state of ^{52}Ca [14], one might naively expect the predominant one-proton knockout to feed the $7/2^-$ ground state of ^{53}Sc through the removal of a single $f_{7/2}$ proton. Experimentally, the measured inclusive cross sections seem to suggest otherwise. An upper limit to the direct population of the ^{53}Sc ground state can be obtained as follows. A single-step knockout reaction is unlikely to populate directly a state with a dominant core-coupled nature, such as the $3/2_1^-$ level, to a significant degree. Hence it is plausible that most if not all of the feeding of the $3/2_1^-$ state comes from higher-lying levels, and an upper limit for the direct population of the $7/2^-$ ground state can be derived from the difference between the inclusive and the $3/2_1^-$ cross sections, that is, $\sigma_{\text{gs}} = \sigma_{\text{inc}} - \sigma_{2.1\text{MeV}} = 6.7(18)$ mb. This extreme situation, where the $3/2^-$ level serves as a "collector" of all higher-state feeding, is depicted in Fig. 3 and leads to the conclusion that in excess of 60% of the inclusive one-proton knockout cross section does not feed the ground state directly.
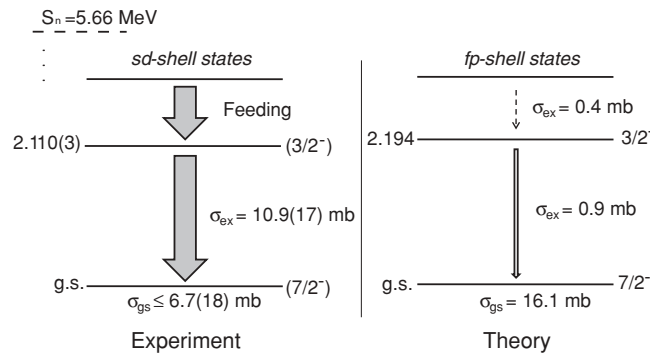
III. DISCUSSION

This emerging experimental picture, where more than 60% of the spectroscopic strength populates excited states rather than the $7/2^-$ ground state, must be confronted with theoretical predictions that combine shell-model spectroscopic factors and single-particle cross sections to yield theoretical partial cross sections. For this purpose, large-scale shell-model calculations in the full fp shell were performed with the OXBASH code [19] using the GXPF1 effective interaction [20]. The results indicate a large overlap between the ground states of ^{54}Ti and ^{53}Sc, with a shell-model spectroscopic factor of $C^2S = 1.85$, close to the total possible $1f_{7/2}$ extreme-single-particle proton occupancy of 2 for ^{54}Ti and negligible spectroscopic strength to any other state (Table I).

Shell-model spectroscopic factors and single-particle cross sections from reaction theory are required to derive theoretical partial cross sections. The single-particle cross sections σ_{sp} were calculated using the spectator-core eikonal model of Tostevin [1,21]. The stripping (inelastic) σ_{str} and diffractive (elastic) σ_{dif} contributions to the single-particle cross section $\sigma_{\text{sp}} = \sigma_{\text{str}} + \sigma_{\text{dif}}$ were computed following the prescription detailed in Ref. [22]. With the single-particle cross sections and the shell-model spectroscopic factors, the theoretical cross sections are calculated with the following equation:

$$\sigma_{\text{th}}(I^\pi) = \left(\frac{A}{A-1}\right)^N C^2S(I^\pi)\sigma_{\text{sp}}[S_p + E_x(I^\pi)], \quad (1)$$

where $[A/(A-1)]^N$ is a center-of-mass correction to the shell-model spectroscopic factors (N is the major oscillator quantum number).

From Table I and Fig. 3, a discrepancy between experiment and theory emerges. In the experiment, most of the knockout cross section populates excited states of ^{53}Sc, while theory, based on shell-model calculations restricted to the fp model space, predicts that nearly all the cross section—about 95%—will proceed to the $7/2^-$ ground state, with negligible amounts

FIG. 3. Comparison of the experimental and theoretical decay strengths of ^{53}Sc in the ^{9}Be(^{54}Ti,^{53}Sc + γ)X reaction. Energies (MeV), J^π values, and the cross sections to the ground and excited states are given. Experimentally, a large, integrated partial cross section to excited states is observed, whereas the shell model predicts a nearly exclusive population of the ground state (see text for details).

TABLE I. Theoretical spectroscopic factors (C^2S), single-particle cross sections (σ_{sp}), and partial cross sections (σ_{th}) to final states in ^{53}Sc for the ^{9}Be(^{54}Ti,^{53}Sc + γ)X knockout reaction (proton separation energy $S_p(^{54}$Ti) = 15.26 MeV). Only states with $C^2S \geqslant 0.01$ are shown. Positive-parity states are outside of the shell-model space used. Because of the uncertainty in the level scheme of ^{53}Sc, only the experimental partial cross section to the ground state could be determined. The factor of 0.4 between the experimental and theoretical partial cross sections to the ground state is in agreement with the systematics for the reduction factors reported in Ref. [22].

E_x (keV)	nlj	C^2S	σ_{sp} (mb)	σ_{th} (mb)	σ_{exp} (mb)
0	$1f_{7/2}$	1.85	8.249	16.2	$\leqslant$6.7(18)
2110	$2p_{3/2}$	0.06	7.845	0.5	–
3221	$1f_{5/2}$	0.01	6.757	0.1	–
3383	$2p_{1/2}$	0.01	7.769	0.1	–
4000	$2s_{1/2}$	–	7.8	–	–
	$1d_{3/2}$	–	5.7	–	–
	sd shell		sum		10.9(17)

of spectroscopic strength proceeding to the $3/2_1^-$ state and higher-lying levels. It is worth noting, however, that there is an approximate factor of 0.4 between the experimental and theoretical partial cross sections to the ground state. This factor is commensurate with the systematics for the reduction of spectroscopic strength established in Ref. [22].

It appears that additional cross section may well originate from processes not considered by theory. For example, the observed distribution of spectroscopic strength suggests that the contributions of knockout from the proton sd shell, which is outside the active shell-model space used here, and beyond the capabilities of available calculations with current knowledge of cross-shell excitations, may be significant.

Support for this interpretation is provided by Ref. [14], in which appreciable strength ($\approx 30\%$) was observed for two-proton knockout to the 3_1^- state in ^{52}Ca, a level with a configuration involving protons from the sd shell. The observed cross section for the population of the 3^- state in ^{52}Ca is several times weaker than the maximum allowed by simple shell-model configurations, and it is assumed that the remaining spectroscopic strength involving sd shell protons resides above the neutron separation energy of $S_n(^{52}$Ca$) = 4.7$ MeV [14].

The importance of sd cross-shell excitations can be gauged further from the study by Doll *et al.* [23] of the ^{50}Ti$(d,{}^3$He$)^{49}$Sc reaction, considering that ^{50}Ti is a semimagic nucleus ($N = 28$), in analogy with ^{54}Ti ($N = 32$). Significant spectroscopic strength to positive parity sd-shell states was reported, in particular, to a 2.23-MeV level [$C^2S(1/2^+, 2s_{1/2}) = 1.40(10)$] and a 2.36-MeV state [$C^2S(3/2^+, 1d_{3/2}) = 3.62(20)$]. These observations suggest that in the case of the ^{9}Be$(^{54}$Ti$, {}^{53}$Sc$ + \gamma)X$ reaction, a sizable fraction—if not all—of the spectroscopic strength to ^{53}Sc excited states can be attributed to proton-hole excitations in the sd shell. The present result, together with the data from [14], quantifies the low-excitation-energy sd-shell spectroscopic strength in this neutron-rich region of the nuclear chart and shows that it is comparable with the less neutron-rich ^{49}Sc.

The inclusive parallel-momentum distribution of the ^{53}Sc knockout residues, which is sensitive to the orbital angular momentum of the removed nucleon [1], is consistent with our interpretation of the presence of sd-shell contributions. Trajectory reconstruction with the position-sensitive focal-plane detectors combined with ion optics and the magnetic field settings of the S800 spectrograph allows the reconstruction of the parallel momentum distribution of ^{53}Sc on an event-by-event basis. Theoretical momentum distributions can be calculated with the same S matrices used to compute σ_{str} and σ_{dif} [24]. The calculated distributions were convoluted with the momentum profile of the incoming ^{54}Ti beam and a rectangular function, accounting for the differential momentum loss throughout the thick target (see Ref. [22] for details).

The experimental parallel momentum distribution (Fig. 4) was fitted with an admixture of contributions from $1f_{7/2}$, $1d_{3/2}$, and $2s_{1/2}$ orbitals (solid line). The relative ratio between f and sd knockout was fixed by the ratio of the experimental partial cross sections to the ground state [6.7(18) mb] and
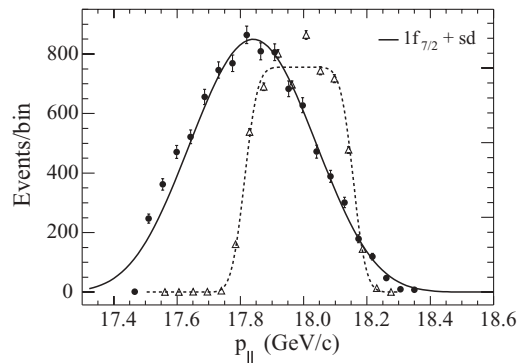

FIG. 4. Momentum profile of the incoming ^{54}Ti beam (triangles) and measured parallel momentum distribution for ^{53}Sc (circles) compared to calculations. The calculation corresponds to 38% $f_{7/2}$ contribution ($\sigma = 6.7$ mb) and 62% sd-shell spectroscopic strength ($\sigma = 10.9$ mb), where $C^2S(d_{3/2})/C^2S(s_{1/2}) = 2$.

excited states [10.9(17) mb], assuming that the strength to the excited states stems in full from proton removal from the sd shell. The sd parallel-momentum distribution was created by weighting the $1d_{3/2}$ and $2s_{1/2}$ distributions by their respective single-particle cross sections [at $E_x = 4$ MeV, $\sigma_{sp}(2s_{1/2}) = 7.8$ mb, and $\sigma_{sp}(1d_{3/2}) = 5.7$ mb], assuming full occupancy. As seen in Fig. 4, the resulting fit is consistent with the removal of protons from both the $f_{7/2}$ orbit and the sd shell. Here we note that, specifically, the high-momentum part of the distribution (>17.6 GeV/c) places the greatest constraint on the ℓ components present. A commonly observed feature of measured longitudinal momentum distributions is a shift of cross section to lower momenta, resulting in a more extended low-momentum tail than predicted by the theoretical sudden, eikonal approximation distributions. The lower momenta of these events are understood as arising from the dissipative stripping mechanism, events in which there is significant energy exchange with the target nucleus. These events are less well described by the (energy nonconserving) sudden approximation calculations. For the case of the one-neutron removal from ^{46}Ar [25], this low-momentum tail was discussed in the framework of such deviations from the eikonal theory used here.

IV. SUMMARY

In summary, in addition to confirming the ground-state transition of the $3/2_1^-$ state and providing a set of newly observed γ rays in ^{53}Sc, the study of the ^{9}Be$(^{54}$Ti$, {}^{53}$Sc$ + \gamma)X$ reaction revealed large cross section yield ($\approx 60\%$) to excited states. These observations are shown to be consistent with the removal of protons from the sd shell. The results highlight the importance of quantitative information on the spectroscopic strengths of sd-shell configurations occurring at fairly low excitation energies: 2.1 MeV in ^{53}Sc. Our results thus stress the need for cross-shell effective interactions for the description of the low-lying nuclear structure in this much-discussed mass region, where the nuclear shell structure is markedly modified by the monopole drift compared to stable nuclei.

[1] P. G. Hansen and J. A. Tostevin, Annu. Rev. Nucl. Part. Sci. **53**, 219 (2003).

[2] A. Gade and T. Glasmacher, Prog. Part. Nucl. Phys. **60**, 161 (2008).

[3] E. K. Warburton, J. A. Becker, and B. A. Brown, Phys. Rev. C **41**, 1147 (1990).

[4] J. R. Terry *et al.*, Phys. Lett. **B640**, 86 (2006).

[5] J. R. Terry *et al.*, Phys. Rev. C **77**, 014316 (2008).

[6] T. Otsuka, R. Fujimoto, Y. Utsuno, B. A. Brown, M. Honma, and T. Mizusaki, Phys. Rev. Lett. **87**, 082502 (2001).

[7] J. I. Prisciandaro *et al.*, Phys. Lett. **B510**, 17 (2001).

[8] R. V. F. Janssens *et al.*, Phys. Lett. **B546**, 55 (2002).

[9] S. N. Liddick *et al.*, Phys. Rev. Lett. **92**, 072502 (2004).

[10] D.-C. Dinca *et al.*, Phys. Rev. C **71**, 041302(R) (2005).

[11] O. Sorlin *et al.*, Nucl. Phys. **A632**, 205 (1998).

[12] H. Crawford *et al.*, Acta Phys. Pol. B **40**, 481 (2009).

[13] S. Bhattacharyya *et al.*, Phys. Rev. C **79**, 014313 (2009).

[14] A. Gade *et al.*, Phys. Rev. C **74**, 021302(R) (2006).

[15] D. J. Morrissey *et al.*, Nucl. Instrum. Methods Phys. Res. B **204**, 90 (2003).

[16] D. Bazin *et al.*, Nucl. Instrum. Methods Phys. Res. B **204**, 629 (2003).

[17] J. E. Yurkon *et al.*, Nucl. Instrum. Methods Phys. Res. A **422**, 291 (1999).

[18] W. F. Mueller *et al.*, Nucl. Instrum. Methods Phys. Res. A **466**, 492 (2001).

[19] B. A. Brown, A. Etchegoyen, and W. D. M. Rae, The computer code OXBASH, MSU-NSCL Report No. 524, 1998 (unpublished).

[20] M. Honma *et al.*, Phys. Rev. C **65**, 061301(R) (2002); Eur. Phys. J. A **25**, 499 (2005).

[21] J. A. Tostevin, J. Phys. G **25**, 735 (1999).

[22] A. Gade *et al.*, Phys. Rev. C **77**, 044306 (2008).

[23] P. Doll *et al.*, J. Phys. G **5**, 1421 (1979).

[24] C. A. Bertulani and P. G. Hansen, Phys. Rev. C **70**, 034609 (2004); C. A. Bertulani and A. Gade, Comput. Phys. Commun. **175**, 372 (2006).

[25] A. Gade *et al.*, Phys. Rev. C **71**, 051301(R) (2005).